JOC The Journal of Organic Chemistry

Article

pubs.acs.org/joc

Conformational Dynamics of *o*-Fluoro-Substituted *Z*-Azobenzene

S. K. Rastogi,[†] R. A. Rogers,[†] J. Shi,[†] C. Gao,[‡] P. L. Rinaldi,[‡] and W. J. Brittain*[,†]

[†]Department of Chemistry and Biochemistry, Texas State University, San Marcos, Texas 78666, United States

[‡]Department of Chemistry, The University of Akron, Akron, Ohio 44325, United States

Supporting Information

ABSTRACT: A conformational analysis of *o*-fluoro *Z*-azobenzene reveals a slight preference for aromatic C−F/π interaction. Density functional theory (DFT) indicates that the conformation with a C−F/π interaction is preferred by approximately 0.3−0.5 kcal/mol. Ground-state conformations were corroborated with X-ray crystallography. (*Z*)-Azobenzene (*Z*-AB) with at least one *o*-fluoro per ring displays ^{19}F−^{19}F through-space (TS) coupling. 2D *J*-resolved NMR was used to distinguish through-bond from TS coupling ($^{TS}J_{FF}$). $^{TS}J_{FF}$ decreases as the temperature is lowered and the multiplets coalesce into broad singlets. We hypothesize that the coalescence temperature (T_c) corresponds to the barrier for phenyl rotation. The experimentally determined barrier of 8−10 kcal/mol has been qualitatively verified by DFT where transition states with a bisected geometry were identified with zero-point energies of 6−9 kcal/mol relative to ground state. These values are significantly higher that values estimated from previous theoretical studies but lie within a reasonable range for phenyl rotation in hydrocarbon systems.

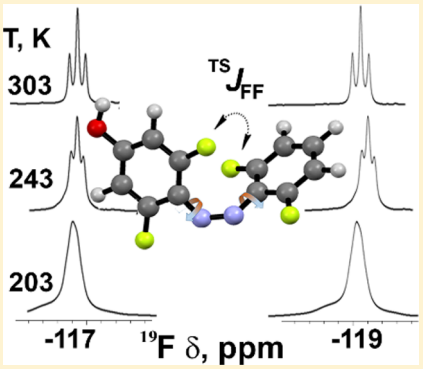

INTRODUCTION

Azobenzene (AB) was first reported in 1834 by Mitscherlich[1] and studied by Nobel in 1856,[2] and its photoisomerization was reported by Hartley in 1937.[3] AB is arguably the most studied organic chromophore in chemistry.[4] AB exists as two geometric isomers with the *E* (*trans*) conformation 12 kcal/mol more stable than the *Z* (*cis*) isomer. The UV−vis absorption spectrum of AB has two absorption bands corresponding to an intense band for $S_0 \rightarrow S_1(\pi-\pi^*)$ transition in the UV and a weaker $S_0 \rightarrow S_2(n-\pi^*)$ transition in the visible region. AB photochromism is principally manifested in changes in ε (molar absorptivity) and modest changes in λ_{max}. Excitation wavelengths for azobenzenes are dependent on the substituents, but generally, irradiation with 320−380 nm promotes *E*- to *Z*-isomerization, and the process is reversed with $\lambda \sim 400-450$ nm exposure or thermally by placing the sample in the dark.

The focus of this report is the dynamic structure of *Z*-AB and the role of phenyl rotation. The structure of *Z*-AB has been determined by X-ray crystallography.[5] *Z*-AB adopts a bent conformation with the phenyl groups twisted ∼53° out of the plane of the azo group (C−N═N−C). There is only one literature report[6] on the experimental determination of phenyl rotation barrier in *E*-AB and none for *Z*-AB. We have previously reported through-space ^{19}F−^{19}F coupling for *o*-fluorosubstituted *Z*-AB.[7] In this study, we combine theory and variable-temperature NMR to determine the phenyl rotation barrier in *Z*-AB systems. We have also observed preferential C−F/π interactions based on X-ray and DFT.

RESULTS

Six compounds are the subject of the present study (Scheme 1). Synthesis and characterization of these compounds has been previously reported.[7]

Scheme 1. Structures of 1−6

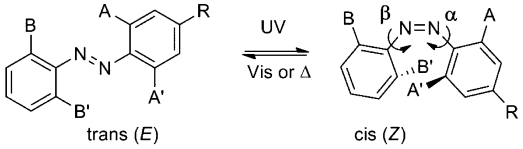

trans (*E*) cis (*Z*)

1: A,B=F, A',B'=H, R=OMe
2: A,B,B'=F, A'=H,R=OMe
3: A,A',B,B'=F, R=OMe
4: A,B,B'=F, A',R=H
5: A,A',B=F, B'=H, R=OMe
6: A'=F, A,B,B',R=H

^{19}F NMR. Peaks for *E*-AB appeared as singlets in the $\{^1H\}^{19}F$ NMR spectrum while coupling was observed in **Z1−5** between *o*-Fs on adjacent rings (Table 1). **Z1−5** are asymmetric ABs in which F_a and F_b are chemically inequivalent. Figure 1 shows the $\{^1H\}^{19}F$ spectrum of a mixture of (*Z*)- and (*E*)-1-(2,6-difluoro-4-methoxyphenyl)-2-(2,6-difluorophenyl)diazene (spectra for **1**, **2**, **4**, and **5** provided as Figures S1−4). ^{19}F peaks for **Z1−6** isomers are shifted downfield relative to the *E* isomer, except for F_a of **Z3**. The multiplicity of the coupling is consistent with rapid phenyl rotation so that either triplet or doublet is observed depending on the number of F's on the adjacent ring.

Received: September 20, 2015
Published: October 27, 2015

DOI: 10.1021/acs.joc.5b02202
J. Org. Chem. 2015, 80, 11485−11490

Table 1. ^{19}F NMR Data for 1−6[a] and Thermodynamics Associated with NMR Coalescence

	δ, ppm (*E*)		δ, ppm (*Z*)		*Z*			
compd	A,A′ (F_a)	B,B′(F_b)	A,A′ (F_a)	B,B′(F_b)	$^{TS}J_{FF}$[c] (Hz)	T_c[d] (K)	ΔG‡[ef] (kcal/mol)	DFT ΔG‡[g] (kcal/mol)
1	−121.31	−125.30	−118.10	−122.26	2.2	−183	9.7	6.3
2	−121.27	−122.80	−119.26	−120.82	4.1	−203	10.6	*h*
3	−117.63	−122.53	−117.77	−119.85	4.8	−203	10.5	7.0, 9.5
4[b]	−121.73	−124.10	−119.75	−122.89	5.9	<−173	8.8	4.9, 7.1
5	−117.59	−124.79	−117.77	−122.69	4.4	nd[i]		
6	−121.70		−118.16					

[a]δ referenced to internal standard, $CFCl_3$ (0.0 ppm). [b]For **4**, F_a = monosubstituted ring. [c]$^{TS}J_{FF}$: through-space ^{19}F−^{19}F coupling. [d]T_c = coalescence temperature. [e]ΔG‡ determined by $k^{-1} = (\sqrt{2}\pi^{TS}J_{FF})$. [f]Variable-temperature NMR performed in CD_2Cl_2, unless otherwise noted. [g]Calculated difference in zero-point energy for putative transition state relative to ground state; two values indicate the energies for two distinct transition-state geometries. [h]Putative transition state did not converge. [i]Not determined.

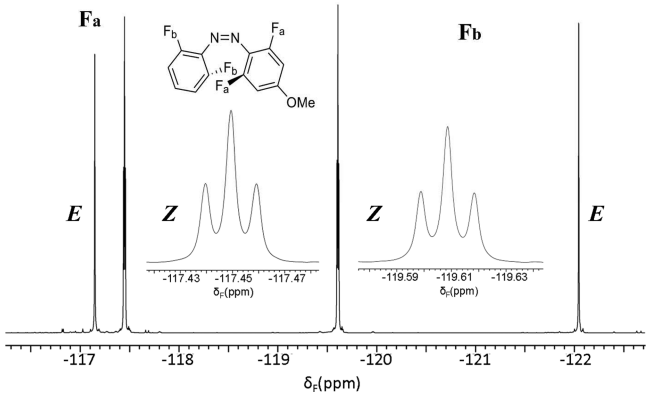

Figure 1. 470 MHz {^{1}H}^{19}F 1D NMR of ***E*3** and ***Z*3**, $CDCl_3/CH_2Cl_2/CCl_4$ (27/60/13), 303 K.

2D *J*-Resolved Characterization. The main peaks in the 2D *J*-resolved NMR spectrum (Figure 2) are triplets for ***Z*3** and singlets for ***E*3**. The splittings in the *Z* isomer are attributed to TS coupling between F_a and F_b (Figure 1). Intraring $^4J_{FF}$ through-bond coupling is not observed because rapid phenyl ring rotation renders two fluorines on the same ring chemically equivalent. Replacement of ^{12}C with ^{13}C on one of the CF carbons shifts the directly attached fluorine upfield by ca. 0.1 ppm, due to an isotope effect,[8] and removes the chemical shift equivalence. The resulting doublets in *F2*, from the F−C−C−^{13}C−*F* isotopomer are shifted upfield and are ca. 1% of the intensities of the main peaks from the pure ^{12}C isotopomer. Half of the doublets (in F_2) are clearly resolved upfield of each main peak, but the downfield half of the doublets fall on the downfield shoulders of the main peaks and are not clearly resolved. In these satellite signals, extra doublet splittings are observed, which are attributed to $^4J_{FF}$ intraring through-bond couplings between the nonequivalent fluorines in F−C−C−^{13}C−F spin systems.

Figure 2 shows the 2D *J*-resolved spectrum of ***Z*3** where multiplicity of the ^{13}C satellites indicates two coupling constants evidenced by doublet of triplets for ***Z*3**. From this spectrum, we have determined that the TS coupling constant is 4.8 Hz and the through-bond coupling is 2.5 Hz. The *E* isomer only displays through-bond coupling. The magnitude of $^{TS}J_{FF}$ (2.2−5.9 Hz) for ***Z*1−5** was relatively low compared to many literature values of $^{TS}J_{FF}$ which were reported for nonfluxional systems with large intramolecular F−F distances (d_{FF}).[9]

Variable-Temperature NMR. Compounds **1**−**4** were studied by low-temperature ^{19}F NMR. The ^{19}F peaks for the *Z* isomer are shifted to lower field (^{19}F peaks for the *E* isomer shifted to higher field) and the multiplets collapsed into a singlet as the temperature was decreased. The coalescence was reversible over repeated cycles. No significant changes in the spectrum were observed above room temperature. We note that both multiplets collapse simultaneously, arguing that the dynamic process underlying the loss of coupling involves both phenyl groups. Figure 3 displays the variable temperature spectra for a mixture of ***Z*3** and ***E*3**. Variable-temperature spectra for ***Z*1**, **-2**, and **-4** are provided in the Supporting Information; compounds ***Z*1−4** displayed qualitatively similar behavior with T_c = 173−203 K. We argue that loss of coupling is not due to line broadening based on line-shape analysis of the *E* isomer with decreasing temperature. We attribute the loss of coupling to a dynamic process. Table 1 contains the

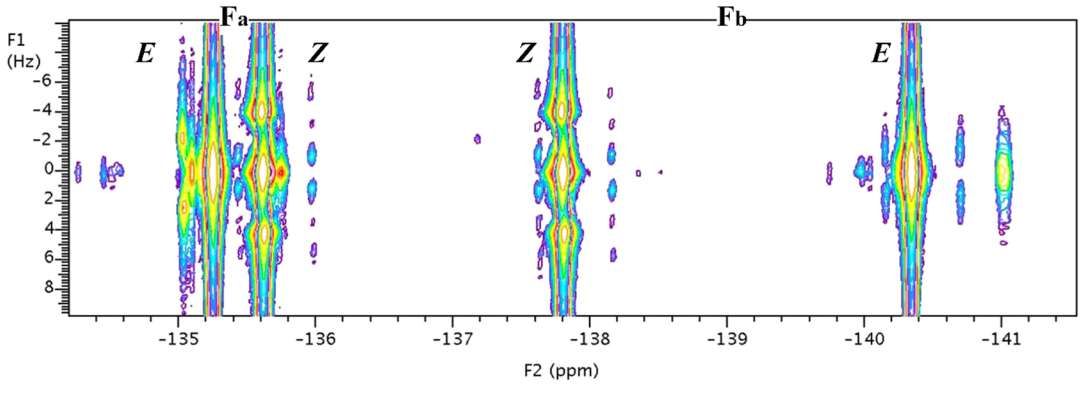

Figure 2. Variable-temperature 470 MHz {^{1}H}^{19}F 2D *J*-resolved NMR of **3**, $CDCl_3/CH_2Cl_2/CCl_4$ (27/60/13), 303 K.

DOI: 10.1021/acs.joc.5b02202
J. Org. Chem. 2015, 80, 11485−11490

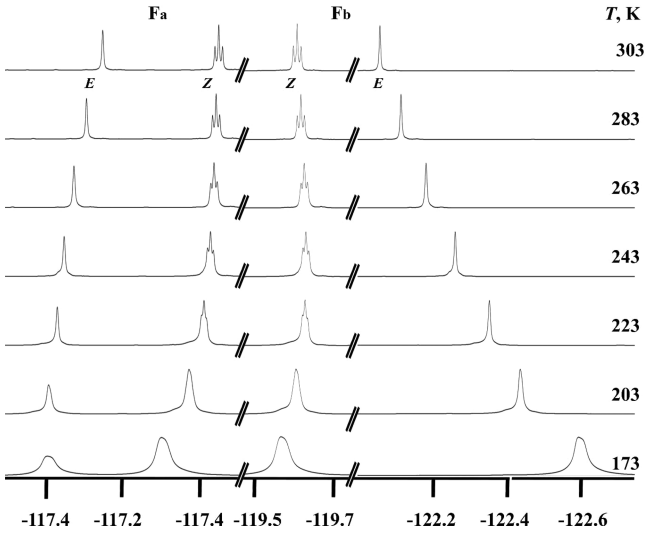

Figure 3. Variable-temperature 470 MHz $\{^1H\}^{19}F$ 1D NMR of **3**, $CDCl_3/CH_2Cl_2/CCl_4$ (27/60/13).

coalescence temperature (T_c) for **Z1**−**4** and the calculated $\Delta G^{\ddagger}$ for a dynamic process. T_c for **Z4** is an upper limit due to limitations in solvent viscosity and the accessible temperature range with the spectrometer prohibited sufficiently low temperatures to observe complete coalescence. The estimated error in calculated $\Delta G^{\ddagger}$ is ±0.3 kcal based on ±5° uncertainty in T_c. Individual $\Delta G^{\ddagger}$ values correspond to the energy difference at T_c.

DFT and X-ray Analysis. There are four possible conformations for *Z*-AB that interchange by phenyl rotation (rotation about dihedrals α and β, Scheme 1). In the parent AB system, these four conformations are equivalent. For **Z1**−**6**, the number of possible conformations depends on the substitution pattern. **Z1** has four ground-state conformations (Supporting Information), and **Z2**−**6** can be characterized by two conformations (Supporting Information). Density functional theory (DFT) (B3YLP/cc-pVTZ) was used to determine the most stable conformation (Figure 4). Also provided in Figure 4

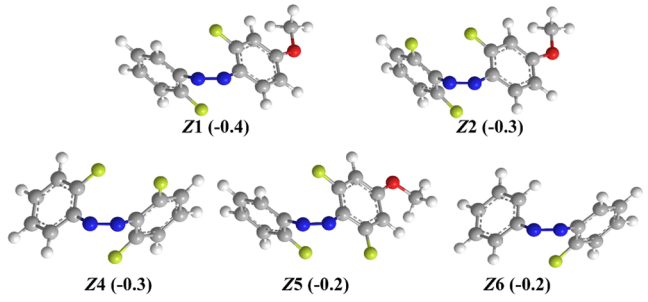

Figure 4. Most stable ground-state conformations of **Z1**,**2**,**4**−**6** based on DFT (ΔZPE, kcal/mol, relative to less stable conformation).

are the zero-point energies relative to the least stable conformation. In all cases, the conformations placing a fluorine over the adjacent aromatic ring were more stable by 0.2−0.4 kcal/mol.[10] Corroboration of this preferred conformation was obtained by X-ray crystallography of **Z2** reported previously[7] and **Z6** (Supporting Information).

The transition states for interconversion of conformations were determined using the Berny algorithim.[11] Correct assignment of transition states was confirmed by frequency analysis; animation of the imaginary frequency revealed a phenyl twisting deformation consistent with the anticipated reaction pathway of phenyl rotation. We identified transition states for **Z1**, **-3**, and **-4** (Figure 5); putative transition-state

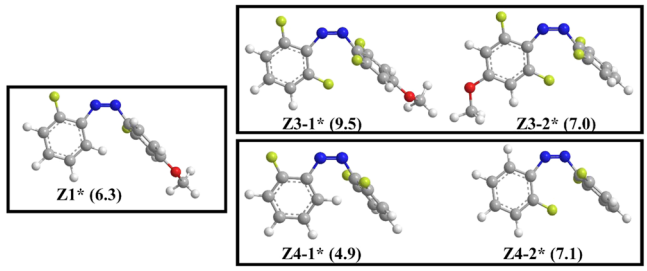

Figure 5. Transition-state structures based on computations using B3YLP/cc-pVTZ. The number is parentheses corresponds to the difference in zero-point energy (sum of electronic and thermal free energies) relative to ground state (in kcal/mol). Computations correspond to 298 K with no solvent model.

structures for **Z2**, **-5**, and **-6** either did not converge or imaginary frequencies did not correspond to vibrations expected for phenyl rotation. The common feature of the identified transition state structures is a bisected geometry in which the plane of the phenyl rings are perpendicular.

DISCUSSION

We report two phenomena in the conformational behavior of *Z*-AB. While the primary focus of this report is the temperature dependence of $^{TS}J_{FF}$, we also report an example of preferential of C−F/π interaction. *Z*-AB is a molecular system with a rich array of possible nonbonded, intramolecular interactions. To fully understand the origin of the observed $^{TS}J_{FF}$, we performed DFT studies of preferred conformations that was augmented by X-ray analysis of those *Z*-AB compounds that could be crystallized. We report that a preferential interaction exists between the aromatic C−F and the adjacent π system.

This effect has been previously documented in the literature, most recently by Ams and co-workers[12] where they observed modest conformational preference (0.1−0.4 kcal/mol) for placing an aliphatic C−F over an aromatic ring. Lectka and co-workers[13] studied the interaction of a bridge-head F with adjacent C═C in a tricyclic norbornane. The X-ray structure of this rigid system shows a nonbonded distance between aliphatic C−F and an adjacent alkene of 268 pm, substantially less than the sum of van der Waals radii (317 pm). This nonbonded interaction also was revealed by through-space $^{13}C-^{19}F$ spin−spin coupling. Lectka et al.[13] observed alkene bond angle distortion, which suggests a repulsive component in this C−F/π interaction. Ho, Chung, and co-workers[14] reported nonbonded interactions in a polycyclic system which placed *o*-fluorines on a phenathrene fragment over flanking phenyl rings. They observed large ^{19}F upfield shifts for rigid systems compared to phenanthrene, which was interpreted as a steric effect on F by interaction with a phenyl ring. Hirao, Hong, and co-workers[15] reported that C−H/π and C−F/π interactions control the conformation of N-heterocyclic carbene palladium complexes. However, the C−F/π interaction involves perfluorophenyl groups; it is well-known that the charge density of C_6F_5 aryl rings is opposite relative to C_6H_5 making an attractive interaction with C−F more reasonable.

DOI: 10.1021/acs.joc.5b02202
J. Org. Chem. 2015, 80, 11485−11490

We hypothesize that the decrease of $^{TS}J_{FF}$ with lower temperature corresponds to the barrier for phenyl rotation. Through-space F−F coupling has been extensively studied, and several empirical formulas for the dependence of $^{TS}J_{FF}$ on the distance between interacting fluorines (d_{FF}) have been developed on the basis of rigid cyclophanes,[16] 1,3-diarylnapthalenes,[17] 1-pentafluorophenyl-1-trifluoromethylethylenes,[18] and naphthalene/phenanthrenes.[19] These empirical formulas can be used to estimate $^{TS}J_{FF}$ from d_{FF} observed in the X-ray structures of **Z2** and **Z4** and from optimized DFT structures of **Z1**−**4**. The average d_{FF} for **Z3** is 420 pm from X-ray and 440 pm by DFT, which corresponds to $^{TS}J_{FF}$ values are 0.2−0.4 Hz based on Ernst's formula[16] and ∼0 Hz using Mallory's formula.[17] The d_{FF} values for **Z2** are 360 pm (X-ray) and 410 pm (DFT) which correspond to $^{TS}J_{FF}$ = 2.6 and 0.5 Hz using Ernst and ∼0 Hz using Mallory's formula. Based on DFT, the average d_{FF} for **Z1**−**4** were in the range of 410−440 pm for the lowest energy conformation. These empirical formulas argue that no $^{TS}J_{FF}$ should be observed in the ground-state conformations, which agrees with the experimental observation of singlets in the low-temperature ^{19}F NMR spectrum. We argue that the observation of $^{TS}J_{FF}$ at room temperature can be explained by a dynamic equilibrium between conformations that sample a variety conformations with unique d_{FF} values, some of which are small enough to induce through-space coupling. For example, **Z1** can be described by four unique conformations (Supporting Information) with ground-state energy differences <0.5 kcal; the value of d_{FF} varies from 340 to 640 pm. The conversion of these conformations requires phenyl rotation. A similar explanation was reported by Xie and co-workers[20] to explain the temperature dependence of ^{13}C−^{19}F and ^{19}F−^{19}F through-space couplings in the conformational dynamics of bis(BF_2)-2,2′-bidipyrrins.

Rotation about dihedral angles α and β (Scheme 1) is a dynamic process where energy scales with the magnitude of dihedral angle change. Complete phenyl rotation with concomitant exchange of the *ortho* substituents occurs at the maximum in a plot of the dihedral angle versus DFT. The ground states of **Z1**−**6** exist in shallow energy wells where dihedral angles (α,β) can vary by ±10° with less than 1 kcal change in zero-point energy (Figure 6). Duarte and co-workers[21] reported that differences in zero-point energy of the parent *Z*-azobenzene were less that 1 kcal for dihedral angles ±15° about the ground-state geometry. This low energy conformational process makes *o*-fluorines on the same ring chemically equivalent in the ^{19}F NMR spectrum which we evaluated by DFT NMR calculations.

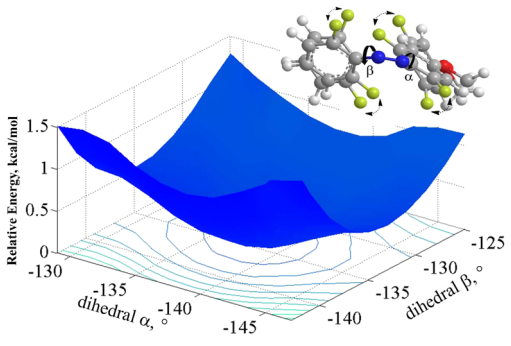

Figure 6. Potential energy scan about ground-state minimum for **Z3** (B3YLP/cc-pVTZ).

Phenyl rotation is rapid at room temperature accounting the observed spin−spin multiplicity in the ^{19}F NMR spectrum and the observation of $^{TS}J_{FF}$ at room temperature. We identified transition states with a bisected geometry (dihedral angles α and β = 0, 90°) using DFT. DFT calculations on transition-state energies (Figure 5) roughly correspond to the experimental values in Table 1. The calculated transition state energies for **Z3**−**1*** and **Z3**−**2*** (Figure 5) differ where the higher energy is associated with rotation of the methoxy-substituted phenyl group consistent with the higher electron density in the methoxy-substituted aromatic ring that should be more repulsive to the bisecting C−F group. However, the experimentally observed collapse of both multiplets at the same temperature argues that both phenyl rotations are suppressed simultaneously and should have similar rotation barriers.[22] Likewise, DFT of **Z4** predicts different phenyl rotation barriers, which is not observed experimentally. As phenyl rotation slows with lower temperature, the equilibria between conformations ceases and effectively leads to a higher average d_{FF} with concomitant decrease in $^{TS}J_{FF}$. Experimental values for $\Delta G^{\ddagger}$ (Table 1) are higher than those predicted from DFT calculations of transition states (Figure 5). However, we argue that DFT qualitatively supports our hypothesis that cessation of phenyl rotation is responsible for loss of spin−spin coupling at lower temperatures. The DFT values in Figure 5 correspond to the gas phase at room temperature. We observed little influence of implicit solvent models in calculated DFT energies. For the Figure 5 transition-state structures, we calculated ZPE values at the corresponding coalescence temperatures: **Z3**−**1*** (9.2 kcal/mol, 203 K), **Z3**−**2*** (3.8 kcal/mol, 203 K), **Z1*** (5.4 kcal/mol, 183 K), **Z4**−**1*** (4.5 kcal/mol, 173 K), and **Z4**−**2*** (6.7 kcal/mol, 173 K).

Our study is the first experimental report on phenyl rotation in *Z*-AB. Klug and Burcl[23] studied rotational barriers in AB and azonaphthalene using DFT (OLYP/cc-pVTZ). For *Z*-AB, they reported a bisected transition state structure for phenyl rotation analogous to our study, but with a much lower stationary point energy of 2.7 kcal/mol. A bisected transition state with the same geometry to our putative transition state in *Z*-AB phenyl rotation was also reported in a computational study (B3YLP/6-31G*) on *E*-*Z* AB photoisomerization.[24] Meier[25] subsequently questioned Klug and Burcl's results and argued calculations should be performed with contribution of nondynamic correlation with a sufficiently large basis set. Other computational reports on studies of AB have focused on the *E*−*Z* photoisomerization and the corresponding stationary point structures.[24,26−29] Klug and Burcl[23] calculated a phenyl rotation barrier of 5.3 kcal for *E*-AB which compares favorably with the results of Konaka (RHF/6-31G** and MP2/6-31+G*)[6] and Chen and Cheih (B3YLP/cc-vVDZ).[29] Konaka experimentally measured a 1.7 kcal/mol barrier in *E*-AB using gas electron diffraction which is several times lower than theory.

Phenyl rotation in *Z*-AB involves both steric and electronic factors principally due to azo conjugation between phenyl rings. Literature examples of experimental barriers (kcal/mol) for phenyl rotation in hydrocarbon systems have been reported: (1) 17.0 for 7-phenyl-7-(2-fluorophenyl)norbornane,[30] (2) 17.1 for 1-(2-fluorophenyl)-8-(2-methylphenyl)naphthalene,[31] (3) 21.0 for 9-phenylanthracene,[32] (4) 7.5 for 2-phenyladamantane,[33] (5) 7.9 for 1-methyl-7,7-diphenylbicyclo[2.2.1]-heptane,[34] (6) 9.8 for 10-methyl-9,11-diphenyl-10-azatetracylco[6.3.0.0^{4,11}0.^{5,9}]undecane,[35] and (7) 16.1 for *N*-benzyl-*N*-*o*-tolyl-*p*-methylbenzenesulfonamide.[36] Our observa-

DOI: 10.1021/acs.joc.5b02202
J. Org. Chem. 2015, 80, 11485−11490

tion of an 8−10 kcal/mol barrier for **Z1−4** phenyl rotation is on the lower end of the 7.9−21.0 kcal/mol range for literature reports and makes sense for a fluxional system.

Our proposed mechanism is based on a "one-ring flip" process. Mislow[37] and Grilli and co-workers[38] have described a "two-ring flip" mechanism for conformational equilibria in systems with two phenyl rings bonded to the same sp^2-hybridized carbon. The transition state for the analogous process in azobenzene would correspond to coplanar phenyl rings orthogonal to the plane of azo bond. DFT estimates of this transition-state structure were consistently in excess of 25 kcal/mol; this result argues against this conformational process. We acknowledge that these literature systems are not fully analogous to AB, which involves conjugative effects in phenyl rotation. We also argue for cautious extension of these results to other AB systems.

CONCLUSIONS

Through-space $^{19}F-^{19}F$ coupling is observed in *o*-fluoro *Z*-AB at room temperature. Based on empirical formulas in the literature, intramolecular distances in the lowest energy conformation of these systems are too large to observe through-space coupling. The highly fluxional nature of these compounds leads to an averaged d_{FF} that can account for the observed NMR coupling at room temperature because higher energy conformations correspond to smaller intramolecular F−F distances. As the sample temperature decreases, $^{TS}J_{FF}$ decreases and we observe collapse of multiplets to broad singlets. This coalescence temperature (T_c) corresponds to barrier for an exchange of *ortho* substituents. Values for $\Delta G^{\ddagger}$ as determined by T_c roughly correspond to ΔZPE for computed transition state structures for phenyl rotation. Our reported experimental values for phenyl rotation in *Z*-AB (8−10 kcal/mol) are significantly higher than that predicted in prior computational work on the parent AB system but fall within a reasonable range for phenyl rotation barriers in hydrocarbon systems.

EXPERIMENTAL SECTION

Unless otherwise noted, all reagents were obtained from commercial sources and used without purification. Synthesis and characterization of **1−6** has been previously reported.[7]

Instrumentation. Absorption measurements were performed using either a scanning or diode array UV−vis spectrometer. For photochemical production of samples enriched in *Z* isomer, we used a 50−200 W Research Arc Lamp; the output was cooled with a water filter and passed through a bandpass filter (350 nm center, 70 nm fwhm). X-ray crystallography was performed on a single-crystal X-ray diffractometer.

^{19}F 1D and ^{19}F homonuclear 2D-J NMR spectra of **3** (at all temperatures) were collected from a 500 MHz spectrometer equipped with five broad band rf channels and a 5 mm $^{1}H/^{19}F/^{13}C$ triple resonance pulse field gradient probe. This probe contains no fluorine-containing materials near the coil in order to avoid the interference from the background fluorine signals that usually exist in the standard probes. The high frequency channel on this probe is doubly tuned to ^{1}H and ^{19}F to produce short 90° pulse widths needed to excite large fluorine spectral windows. A duplexer with low insertion loss provides the capability of combining the signals from the ^{1}H and ^{19}F rf channels and direct them to the dual-tuned $^{1}H/^{19}F$ high frequency channel of the probe. The returning ^{1}H and ^{19}F signals from the probe can be separated by this duplexer again and the desired signal (^{1}H or ^{19}F) directed to the receiver. The sample of **3** was prepared by dissolving approximately 10 mg of material in a solvent mixture of $CDCl_3/CH_2Cl_2/CCl_4$ (27/60/13) (v/v/v) with a trace of $CFCl_3$ added as a chemical shift reference.

^{19}F 1D NMR spectra of **1**, **2**, and **4−6** (at all temperatures) were obtained using a 400 MHz spectrometer. ^{19}F shifts are relative to internal $CFCl_3$ (0.0 ppm), and all reported spectra were obtained with broadband ^{1}H decoupling. Room-temperature samples were measured in $CDCl_3$, and variable-temperature experiments were measured in CD_2Cl_2. The probe temperature was calibrated using a methanol thermometer. Spectra were typically acquired with a digital resolution of 0.1 Hz/pt.

Computational Details. Density functional theory (DFT) calculations were performed with the cc-pVTZ basis set and the restricted B3YLP as implemented in Gaussian 09.[39] Our choice of the cc-pVTZ basis set was based on work of Duarte et al.[22] and Klug and Burcl.[23] We also performed comparative computations using MP2 (Möller−Plesset perturbation theory) with 6-311++G(d,p) basis set, the long-range corrected WB97XD functional combined with 6-311++G(d,p) basis set and B3LYP/6-311++G(d,p). Our choice of B3LYP/cc-pVTZ was chosen because it best matched the X-ray structural parameters for **Z2** and **Z3**. Geometry optimizations and frequency calculations were performed in the gas phase at room temperature, unless otherwise noted. Additional calculations were performed at the observed coalescence temperature for each system using the temperature option in G09. Ground- and transition-state energies are zero-point energies (Sum of Electronic and Thermal Free Energies in G09 output). Vibrational analysis was used to confirm the ground-state (0 imaginary frequencies) and transition-state (1 imaginary frequency) structures. Transition-state structures were identified and confirmed by a multistep process: (1) potential energy scans about CCNN dihedrals, (2) geometry optimization while holding dihedral angle at fixed value until desired level of theory converges with Berny algorithm,[11] (3) unconstrained geometry optimization, and (4) frequency analysis. NMR calculations of ^{19}F chemical shifts followed the procedure of Lectka et al.[13]

ASSOCIATED CONTENT

Supporting Information

The Supporting Information is available free of charge on the ACS Publications website at DOI: 10.1021/acs.joc.5b02202.

X-ray structure of **Z6** (CIF)
NMR spectra and computational data (PDF)

AUTHOR INFORMATION

Corresponding Author

*E-mail: wb20@txstate.edu.

Notes

The authors declare no competing financial interest.

ACKNOWLEDGMENTS

W.J.B. thanks the National Science Foundation (PREM Center for Interfaces, DMR-1205670), National Science Foundation REU (CHEM-1156579), and the ACS Petroleum Research Fund (51997UR7) for financial support of this research. We also acknowledge the support of the National Science Foundation for X-ray and NMR instrumentation (CR1IF:-MU-0946998 and MRI-0821254) and the Welch Foundation (AI-0045).

DEDICATION

Dedicated to Professor John D. Roberts on the occasion of his 97th birthday—who taught that physical organic chemistry is not unidirectional but the umbrella of possibilities.

REFERENCES

(1) Mitscherlich, E. *Ann. Pharm.* **1834**, *12*, 311−314.

DOI: 10.1021/acs.joc.5b02202
J. Org. Chem. 2015, 80, 11485−11490

(2) Nobel, A. *Liebigs Ann. Chem.* **1856**, *98*, 253−256.
(3) Hartley, G. S. *Nature* **1937**, *140*, 281−281.
(4) (a) Beharry, A. A.; Woolley, G. A. *Chem. Soc. Rev.* **2011**, *40*, 4422−4437. (b) Bandara, H. M. D.; Burdette, S. C. *Chem. Soc. Rev.* **2012**, *41*, 1809−1825.
(5) Mostad, A.; Romming, C. *Acta Chem. Scand.* **1971**, *25*, 3561−3568.
(6) Tsuji, T.; Takashima, H.; Takeuchi, H.; Egawa, T.; Konaka, S. *J. Phys. Chem. A* **2001**, *105*, 9347−9553.
(7) Rastogi, S. R.; Rogers, R. A.; Shi, J.; Brown, C. T.; Salinas, C.; Martin, K. M.; Armitage, J.; Dorsey, C.; Chun, G.; Rinaldi, P.; Brittain, W. J. *Magn. Reson. Chem.* **2015**, DOI: 10.1002/mrc.4327.
(8) Tordeux, M.; Magnier, E.; Guidotti, J.; Diter, P.; Wakselman, C. *Magn. Reson. Chem.* **2004**, *42*, 700−703.
(9) Hierso, J.-C. *Chem. Rev.* **2014**, *114*, 4838−4867.
(10) These small energy differences should be viewed as approximate. Energy values <1 kcal/mol are difficult to resolve across functionals, and we cannot assert that we fully explored all methods. X-ray data argues for a preferential effect in the crystal, but quantifying the magnitude of the effect in solution is difficult.
(11) Schlegel, H. B. *J. Comput. Chem.* **1982**, *3*, 214−218.
(12) Ams, M. R.; Fields, M.; Grabnic, T.; Janesko, B. G.; Zeller, M.; Sheridan, R.; Shay, A. *J. Org. Chem.* **2015**, *80*, 7764−7769.
(13) Scerba, M. T.; Bloom, S.; Haselton, N.; Siegler, M.; Jaffe, J.; Lectka, T. *J. Org. Chem.* **2012**, *77*, 1605−1509.
(14) Chang, Y.-Y.; Ho, I.-T.; Ho, T.-L.; Chung, W.-S. *J. Org. Chem.* **2013**, *78*, 12790−12794.
(15) Xu, X.; Pooi, B.; Hirao, H.; Hong, S. H. *Angew. Chem.* **2013**, *125*, 1−6.
(16) Ernst, L.; Ibrom, K. *Angew. Chem., Int. Ed. Engl.* **1995**, *34*, 1881−1882.
(17) Mallory, F. B.; Mallory, C. W.; Butler, K. E.; Lewis, M. B.; Xia, A. Q.; Luzik, E. D., Jr.; Fredenburgh, L. E.; Ramanjulu, M. M.; Van, Q. N.; Francl, M. M.; Freed, D. A.; Wray, C. C.; Hann, C.; Nerz-Stormes, M.; Carroll, P. J.; Chirlian, L. E. *J. Am. Chem. Soc.* **2000**, *122*, 4108−4116.
(18) Hilton, J.; Sutcliffe, L. H. *Spectrochim. Acta* **1976**, *32A*, 201−213.
(19) de Azua, M. C. R.; Diz, A. C.; Giribert, C. G.; Contreras, R. H.; Rae, I. D. *Int. J. Quantum Chem.* **1986**, *30*, 585−601.
(20) Xie, X.; Yuan, Y.; Kruger, R.; Broring, M. *Magn. Reson. Chem.* **2009**, *47*, 1024−1030.
(21) Duarte, L.; Fausto, R.; Reva, I. *Phys. Chem. Chem. Phys.* **2014**, *16*, 16919−16930.
(22) A reviewer suggested that the difference in transition-state energies could be also explained by consideration of quinoidal resonance forms. The lower energy for **Z3**-2* could be due to contributions from this resonance structure, which is supported by a shorter N═N−C−C bond length for the methoxy-substituted phenyl in **Z3-2*** relative to **Z3-1***.
(23) Klug, R.; Burcl, R. *J. Phys. Chem. A* **2010**, *114*, 6401−6407.
(24) Dokic, J.; Gothe, M.; Wirth, J.; Peters, M. V.; Schwarz, J.; Hecht, S.; Sallfrank, P. *J. Phys. Chem. A* **2009**, *113*, 6763−6773.
(25) Meier, R. J. *J. Phys. Chem. A* **2011**, *115*, 3604−3604.
(26) Biswas, N.; Umapathy, S. *J. Phys. Chem. A* **1997**, *101*, 5555−5566.
(27) Crecca, C. R.; Roitberg, A. E. *J. Phys. Chem. A* **2006**, *110*, 8188−8203.
(28) Gagliardi, L.; Orlandi, G.; Bernardi, F.; Cembran, A.; Garavelli, M. *Theor. Chem. Acc.* **2004**, *111*, 363−372.
(29) Chen, P. C.; Chieh, Y. C. *J. Mol. Struct.: THEOCHEM* **2003**, *624*, 191−200.
(30) Martinez, A. G.; Barcina, J. O.; de Fresno Cerezo, A.; Gutierrez, R. *J. Am. Chem. Soc.* **1998**, *120*, 673−679.
(31) Annunziata, R.; Ponzini, F.; Raimondi, L. *Magn. Reson. Chem.* **1995**, *33*, 297−307.
(32) Nikitin, K.; Muller-Bunz, H.; Ortin, Y.; Muldoon, J.; McGlinchey, M. J. *Org. Lett.* **2011**, *13*, 256−259.
(33) Schaefer, T.; Beaulieu, C.; Sebastin, R. *Can. J. Chem.* **1991**, *69*, 503−508.
(34) Casarini, D.; Grilli, S.; Lunazzi, L.; Mazzanti, A. *J. Org. Chem.* **2004**, *69*, 345−351.
(35) Gribble, G. W.; Switzer, F. L.; Bushweller, J. H.; Jewett, J. G.; Brown, J. H.; Dion, J. L.; Bushweller, C. H.; Byrn, M. P.; Strouse, C. E. *J. Org. Chem.* **1996**, *61*, 4319−4327.
(36) Maciejewska, D.; Jakowski, J.; Kleps, J.; Chalasinski, G. *J. Mol. Struct.: THEOCHEM* **2004**, *680*, 5−13.
(37) Mislow, K. *Acc. Chem. Res.* **1976**, *9*, 26−33.
(38) Grilli, S.; Lunazzi, L.; Mazzanti, A.; Casarini, D.; Femoni, C. *J. Org. Chem.* **2001**, *66*, 488−495.
(39) Frisch, M. J.; Trucks, G. W.; Schlegel, H. B.; Scuseria, G. E.; Robb, M. A.; Cheeseman, J. R.; Scalmani, G.; Barone, V.; Mennucci, B.; Petersson, G. A.; Nakatsuji, H.; Caricato, M.; Li, X.; Hratchian, H. P.; Izmaylov, A. F.; Bloino, J.; Zheng, G.; Sonnenberg, J. L.; Hada, M.; Ehara, M.; Toyota, K.; Fukuda, R.; Hasegawa, J.; Ishida, M.; Nakajima, T.; Honda, Y.; Kitao, O.; Nakai, H.; Vreven, T.; Montgomery, J. A., , Jr.; Peralta, J. E.; Ogliaro, F.; Bearpark, M.; Heyd, J. J.; Brothers, E.; Kudin, K. N.; Staroverov, V. N.; Kobayashi, R.; Normand, J.; Raghavachari, K.; Rendell, A.; Burant, J. C.; Iyengar, S. S.; Tomasi, J.; Cossi, M.; Rega, N.; Millam, N. J.; Klene, M.; Knox, J. E.; Cross, J. B.; Bakken, V.; Adamo, C.; Jaramillo, J.; Gomperts, R.; Stratmann, R. E.; Yazyev, O.; Austin, A. J.; Cammi, R.; Pomelli, C.; Ochterski, J. W.; Martin, R. L.; Morokuma, K.; Zakrzewski, V. G.; Voth, G. A.; Salvador, P.; Dannenberg, J. J.; Dapprich, S.; Daniels, A. D.; Farkas, O.; Foresman, J. B.; Ortiz, J. V.; Cioslowski, J.; Fox, D. J *Gaussian 09, Revision A.1*; Gaussian, Inc.: Wallingford, CT, 2009.

DOI: 10.1021/acs.joc.5b02202
J. Org. Chem. 2015, 80, 11485−11490